Journal of MATERIALS RESEARCH

Introduction
DOI:10.1557/s43578-021-00293-4

MULTISCALE MATERIALS MODELING OF INTERFACE-MEDIATED THERMOMECHANICAL BEHAVIOR

FOCUS ISSUE

Multiscale modeling of interface-mediated mechanical, thermal, and mass transport in heterogeneous materials: Perspectives and applications

Liming Xiong[1,a], Youping Chen[2], Irene J. Beyerlein[3,4], David McDowell[5,6]

[1] Department of Aerospace Engineering, Iowa State University, Ames, IA 50011, USA
[2] Department of Mechanical and Aerospace Engineering, University of Florida, Gainesville, FL 32611, USA
[3] Department of Mechanical Engineering, University of California, Santa Barbara, CA 93106, USA
[4] Materials Department, University of California, Santa Barbara, CA 93106, USA
[5] School of Materials Science and Engineering, Georgia Institute of Technology, Atlanta, GA 30332, USA
[6] G.W. Woodruff School of Mechanical Engineering, Georgia Institute of Technology, Atlanta, GA 30332, USA
[a] Address all correspondence to this author. e-mail: lmxiong@iastate.edu

Received: 23 June 2021; accepted: 28 June 2021; published online: 7 July 2021

In this perspective, we: (a) characterize the multiscale nature of the mechanical (plasticity, fracture, twinning, and phase transformations) and thermal behavior, as well as the mass transport behavior in a variety of materials with microstructure complexities; (b) examine the applicability of several representative experimental/computational techniques/approaches in identifying the mechanisms underlying the interface-dictated mechanical, thermal, and mass transport; (c) highlight the need for the development of multiscale methods that can address atomistic and continuum descriptions of materials within one framework, together with our preliminary attempts in this regard. This perspective, together with the relevant papers collected in this focus issue, will inspire researchers to further develop advanced theories, algorithms, and software implementation for bottom-up predictive simulation of the deformation, thermal, and diffusion behavior of advanced materials. Such methods can support the design and development of materials with desired combinations of properties, for example high strength/ductility/toughness, low/high thermal/ionic conductivity, corrosion-/irradiation-resistance.

Introduction

Traditional engineering structural materials, such as steels or Ti-6Al-4V alloys (Fig. 1a) [1], and many recently developed materials, such as bulk nanolayered metallic composites [2–5], semiconductor or oxide superlattices [6–13], contain a high number density of interfaces, including grain boundaries (GBs) and/or phase boundaries (PBs), characterized by incoherent, semi-coherent, and coherent interfaces. The presence of those interfaces introduces characteristic length scales that comprise material microstructure. For instance: (i) in polycrystalline Ti-6Al-4V, the micrometer-sized columnar/equiaxed grains (average grain size: ~300 μm) [1] and submicron-sized α-/β-laths are separated by a high density of atomically structured GBs, PBs, and triple junctions (Fig. 1a); (ii) in a typical oxide superlattice, $BaTiO_3/SrTiO_3$, synthesized from epitaxial beam growth, the spacing between the dislocations in the interface misfit dislocation network at the semi-coherent interface varies from several microns down to a few nanometers [9] (Fig. 1b). When such multilevel microstructures are exposed to extreme environments, such as imposed significant plastic deformation, a sudden temperature change (e.g., heat pulse), or a cyclic electrochemical charge, the dislocation slip, phonon-mediated heat flow, interstitial ion diffusion-induced mass transport and even a coupling of them will occur. Their interaction with internal material interfaces may lead to a series of structure changes (twinning, phase transition (PT), fracture, etc.) also spanning a wide range of length scales. This is evidenced by: (1) the formation of a μm-level pileup with a stress concentration at its tip when a queue of dislocations is blocked by a GB or PB, If this high local stress cannot be fully relieved by cross-slip, atomic-level slip transfer, twinning or PT (Fig. 1c) nucleation, variant selection and growth, may be then activated [14–22]; (2) the

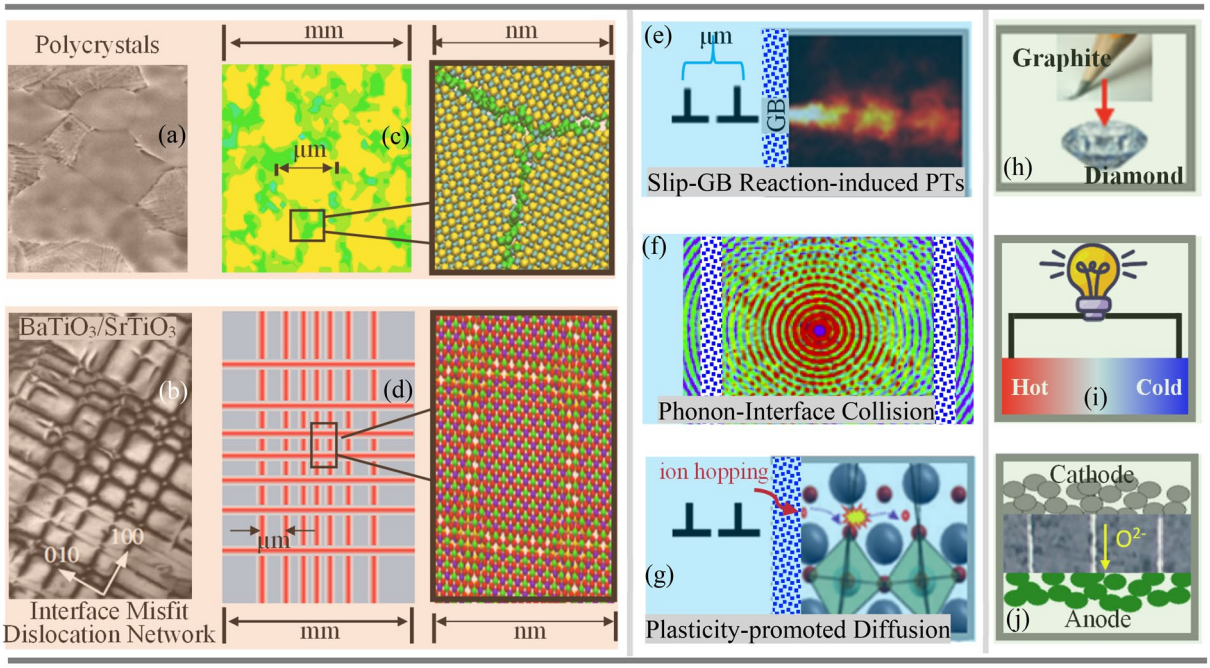

Figure 1: Microstructure of materials containing interfaces and its response to mechanical, thermal, and chemical driving forces: (a–d) the multilevel microstructure of polycrystalline Ti-6Al-4V and $BaTiO_3/SrTiO_3$ superlattices; (e–f) dislocation slip, phonon wave propagation, twinning, PTs, ion hopping and their interactions with the interfaces; (h–j) a manipulation of the interface-mediated mechanical, thermal, and mass transport toward various applications.

atomic scale structure reconfiguration of an interface, e.g., GB, during a phonon-GB collision when a heat pulse-induced phonon wave packet (wave packet size: μm; wavelength: nm) impinges (Fig. 1d) [23–25]; (3) the atomic-level ion hopping promoted by the nanoscale oxygen octahedron (noted as OCT in Fig. 1e) tilting under the high local stress induced by a μm-level dislocation pileup at the interfaces in oxides [26–34]. Obviously, for heterogeneous materials with a high density of interfaces, both the microstructure and its responses to mechanical, thermal, or chemical driving forces are all multiscale in nature, necessitating modeling techniques with diverse resolutions ranging from the atomistic to the micrometer level. Such multiscale methodologies/techniques will enable the researcher to test one hypothesis: with a fine control of the plastic strain and the material's microstructure, the interface-mediated thermomechanical behavior can be manipulated to promote desired properties or responses. These responses may include favorable PTs, suppression of heat flow, and enhancement of ionic transport to achieve, for example: (a) a graphite-to-diamond PT in cold-compressed graphite [35] at low pressure without using catalysts (Fig. 1h); (b) a performance enhancement of thermoelectric materials converting heat flow into electricity [36] (Fig. 1i); (c) a fast ionic transport in plastically deformed oxides for low-temperature fuel cell applications [26–34, 37] (Fig. 1j).

To meet this need for bottom-up control toward manipulating properties, a popular approach is to leverage the synergy of versatile experimental techniques, each of which is at a specific resolution, to characterize certain microstructure and behavior at particular length scales, respectively, to achieve a full length-scale understanding of the behavior of interest. For instance: (i) to understand how the plasticity flow occurs in polycrystalline metals or in multilayered metallic composites at the microscale, the electron backscattered diffraction (EBSD) technique together with the digital image correlation (DIC) can be used to measure microstructure evolution in the vicinity of strain localization near the slip-interface intersection [38–43]. At the nanoscale or the atomic scale, transmission electron microscopy (TEM) or high-resolution TEM (HR-TEM) can be then deployed [44, 45] to resolve the detailed slip-interface reaction process (cross-slip, transmission, absorption, and many others); **(ii)** to gain insights into the nature of phonon-mediated thermal transport across the material interface, a technique referred as the time domain thermoreflectance (TDTR) may be used to first measure the overall thermal conductance of interfaces [46]. As a supplement, an ultrafast pump–probe technique, utilizing ultrafast laser pulses, can be then deployed to achieve extremely fine temporal and spatial resolution at the interface for imaging the detailed phonon scattering process [24, 47–51]; and similarly, (iii) to correlate the material microstructure with its ionic transport properties, electrochemical impedance spectroscopy (EIS) experiments are often conducted to measure the ionic conductivity [52–54]. If desired, the result from EIS can be then correlated with the interface ion diffusion

kinetics, which is usually extracted from the secondary-ion mass spectrometry (SIMS) [55, 56].

These sorts of experimental methods have of course provided researchers with valuable knowledge on how interfaces mediate mechanical, thermal, and mass transport behavior in heterogeneous materials, but are still limited in several aspects: (a) many of them are based on either surface analysis, e.g., EBSD, which only collect data on sample surfaces instead of probing the in situ behavior at a buried interface, or foil analysis (TEM or TDTR), which requires the samples to be sufficiently thin and does not consider the effect of the complex microstructure environment on the interface-mediated thermomechanical behavior; (b) each experimental technique has its own spatial–temporal domain of suitability, none of which can simultaneously resolve the μm-level dislocation plasticity, nanoscale phonon dynamics and the atomic scale ion diffusion, which act together to contribute to the interface-mediated thermomechanical behavior; (c) several key quantities, such as local stress and heat flux at the interface, are usually not directly measured in experiments. Instead, they are calculated from the strain measurement in EBSD/TEM and the temperature gradient in TDTR, respectively, using phenomenological constitutive rules such as Hooke's law [42, 43] and Fourier's law [24] in particular. Moreover, like computational models, experiments have uncertainty both in terms of sensor outputs, processing, and conceptual models that translate measurements into properties. These limitations lead to a series of un-answered questions: Will the mechanical, thermal and mass transport behavior near an interface embedded within a complex microstructure largely differ from that of an isolated interface? If yes, how does the microstructure-induced internal stress contribute to such differences? Is it possible to directly quantify the internal stress/heat flux at the buried materials interfaces rather than measuring the strain/temperature gradient and then converting them into stresses/heat flux according to the empirical constitutive laws? Would it be possible to establish and even manipulate the correlation between the local dislocation density, internal stress intensity factor, twinning/PT nucleation/growth, variant selection, thermal resistance and ion diffusivity? Clearly, answering these questions through experiments alone is extremely challenging, if even possible. Multiscale computer simulations are essential to augment such experimental information to mitigate experimental uncertainties of various forms, including limited regimes of responses and a priori assumption of specific theories or mechanisms, as well as high cost.

Perspectives on the development of multiscale materials modeling methodologies

Researchers have made considerable progress on the development of multiscale modeling methodologies over the past twenty years [57–64]. Multiscale methods generally fall into two categories: sequential and concurrent approaches. In sequential approaches, the pertinent information is extracted from atomistically resolved simulations, e.g., molecular dynamics (MD) or density functional theory (DFT) calculations. This information is then used to inform higher length-scale models, such as dislocation dynamics (DD) [65–71], Boltzmann transport equation (BTE) [72–74], Poisson's equation of diffusion [75–77] (Fig. 2a–c), and among many others. With the atomistic nature of materials being smeared out, such atomistically informed continuum approaches enable an appreciable gain in computational efficiency compared with MD or DFT. The calibration of constitutive rules through fine-scale simulations is, however, non-trivial, especially when a predictive description on how dislocation plasticity, heat and mass flows across the buried interface is concerned. One main reason is that, due to the high computational cost, the periodic simulation cell size in a typical MD model using modest computational resource is usually limited to less than hundreds of nanometers. As a consequence, it can: (i) only accommodate a few dislocations very near the interface and cuts off the μm-level long-range stresses induced by a high density of dislocations accumulation at the interfaces (Fig. 2d); (ii) only allow for nanometer-long-wavelength phonon propagation in small samples and cut off long-wavelength phonons that significantly contribute to the thermal conductivity of superlattices or thin films (Fig. 2e); (iii) only retain the atomistic structures of equilibrium GBs or misfit dislocation networks composed of periodic structure units and cut off the long-range structure heterogeneity of non-equilibrium interfaces, such as the non-equilibrium GB [78] (Fig. 2f).These limitations cast doubts on using atomic-level simulations to extrapolate to the continuum-level constitutive models for practical applications. It renders many sequential approaches not fully predictive when applied for simulating the interface-mediated thermomechanical behavior in engineering materials with coarser scales of microstructure heterogeneity.

In contrast, concurrent methods, such as the Quasicontinuum (QC) [57], coupled length-scale (CLS) approach [58], bridging domain method (BDM) [59], coupled atomistic and dislocation dynamics (CADD) [60], and among many others [61–64], combine atomistic and continuum description in one model. These approaches can accommodate the long-range stress field at the continuum level and also resolve the atomistic structures of critical regions, such as material interfaces. They offer researchers unique platforms for modeling the interface-mediated thermomechanical behavior under the effect of long-range stress fields, which can be evidenced by a series of benchmark examples demonstrating the applicability of those methods in the literature. However, it should be noted that, in most of these models, the atomistic domain fundamentally differs from classical continuum domain in two main aspects: (a) in the atomistic domain, an interatomic potential is used to govern

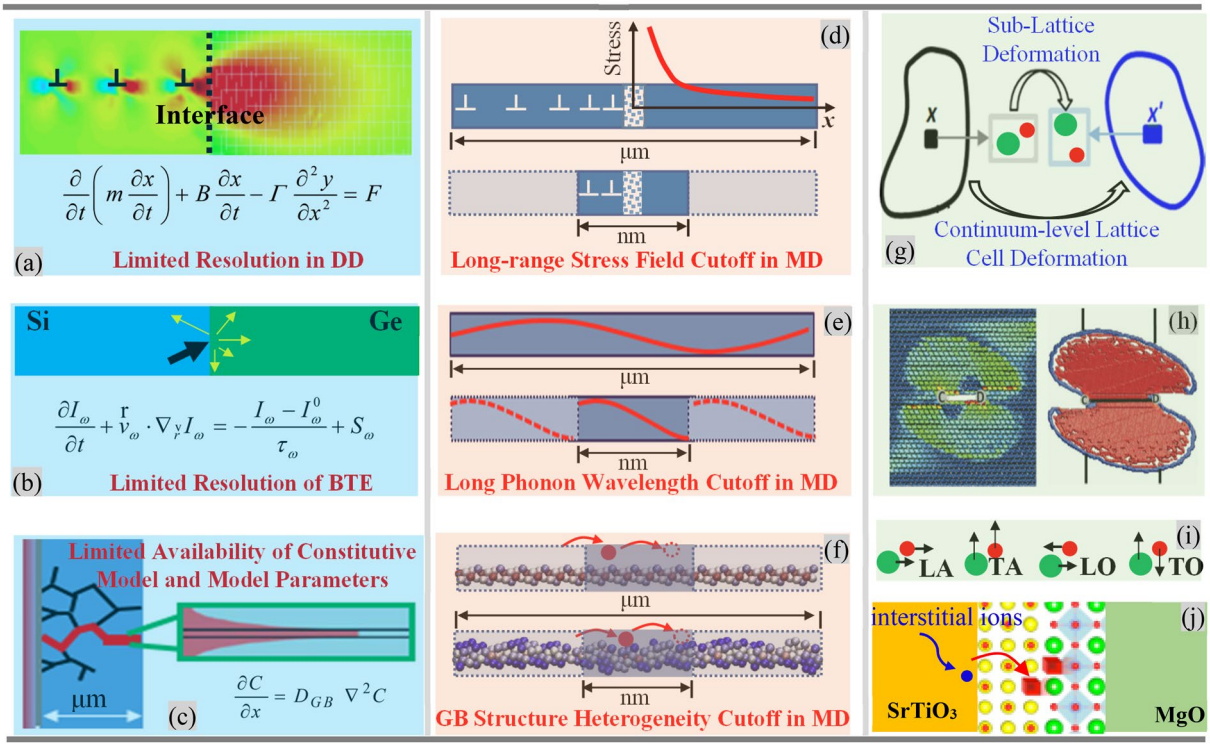

Figure 2: A summary of continuum, atomistic, and a concurrent atomistic-continuum (CAC) model: (a–c) the continuum theories and computer models for simulating dislocation plasticity, phonon transport, and diffusion; (d–f) the atomic-level MD models cutting off the long-range stress field, long-wavelength phonons and the GB structure heterogeneity; (g–j) an atomistic field formulation [79–86], the resulting CAC model and its unique features in accommodating dislocations [87–93], cracks [94–96], full sets of phonons [97–100] (LA, TA, LO, and TO are longitudinal acoustic, transverse acoustic, longitudinal optic, and transverse optic, respectively), and interstitial diffusion in continuum.

the material's behavior, which is non-linear, non-local and give rise to full branches of dispersive phonon dynamics. Instead, the constitutive relation used in the classical continuum domain of those models is linear, local and only gives rise to a limited set of non-dispersive phonon branches; (b) the material defects, e.g., interstitials, vacancies, dislocations, cracks, and many others, can be all naturally allowed in an atomistic domain, but are treated at a lower resolution in the continuum domain. For example, in CADD, the dislocations in the continuum domain are considered as line segments, which have no core structure and interact with each other through the long-range stresses according to the theory of elasticity. In a concurrent model, which combines BDM and extended finite element method (XFEM) [101], the dislocations or cracks are enabled in the continuum domain by introducing a Heaviside step function for capturing the discontinuity across the pre-defined slip or cleavage planes. Due to the above mismatches, an extensive effort has been devoted to constructing a transition region for handshaking atomistic with continuum. For instance, in a QC simulation of the dislocation-GB interaction [102], the finite elements (FEs) in the continuum domain were adaptively refined to fully atomistic along the dislocation migration path, even well away from the GB. Such adaptive refinement removes much of the computational advantage sought by a continuum model. Alternatively, in CADD, a "detection band" to transfer dislocations between atomistic and DD was adopted [60]. The construction of it for curved dislocations in 3D is non-trivial and was not attempted until recently [103–105]. Overall, an inconsistency between atomistic and classical continuum description of materials gives rise to challenges for many concurrent methods when applied for understanding the interface-mediated mechanical, thermal, and mass transport behavior from the bottom-up.

Distinct from the multiscale approaches above, a concurrent atomistic-continuum (CAC) method [87–100, 106–110] was developed over the past decade. Fundamental to CAC is a formulation that unifies atomistic and continuum description of materials [79–86]. This formulation generalizes Kirkwood's statistical theory of transport [111–114] by including a two-level description of crystals. It considers material as a collection of continuously distributed lattice cells, within each of which a group of atoms is embedded (Fig. 2g). The atomic displacement field is then expressed as the sum of a continuum-level lattice cell deformation and a discrete sublattice deformation. In this way, the continuum field quantities (mass, energy, and stress) can be defined in terms of atomic-level variables (forces, displacement, and velocities) [79–82].

The atomistic-decorated balance equations [83, 84] were then derived. They are identical in form to the balance equations in continuum theories. Thus, continuum modeling techniques, such as the FE method, can be used to solve them. The discretization of a sample into FEs leads to a unique coarse-grained (CG) description of materials: (1) it is non-local and nonlinear in nature by using the interatomic potential as the only constitutive rule; (2) the FE in it conforms to the geometry of a material's primitive cell [87, 94]. This element ensures that dislocations/cracks can migrate along the FE boundaries, which are along the slip/cleavage planes [87–96] (Fig. 2h); (3) it retains the full spectrum of dispersive phonon dynamics by allowing various phonon modes [97–100] (Fig. 2i); (4) it allows interstitial ion hopping in the FE domain where the interstitial sites have been built in (Fig. 2j). A combination of such unique CG descriptions with fully atomistic bases leads to a CAC model that can be well suited for bottom-up simulation of μm-level plasticity, heat, and mass flow across atomistically resolved interfaces. The applicability of such a concurrent multiscale model approach to support the understanding of dislocation plasticity, fracture, twinning, PTs, thermal transport, diffusion, and their interactions in a variety of heterogeneous materials containing GBs, PBs, and other interfaces is discussed and analyzed in detail in the following.

Perspectives on the applications of multiscale material modeling methodologies

It is widely accepted that the factors or phenomena that affect many mechanical behaviors of materials, such as plasticity, creep, fatigue, damage, and facture, all span a broad range of length scales. As a sample demonstration, the multiscale nature of slip transfer in polycrystalline Ti alloys (Fig. 3a–c), fracture of multiphase aggregates (Fig. 3d–f), and plastic flow in multilayered metallic composites (Fig. 3g–i) are analyzed in detail. Figure 3a shows the image of a plastically deformed polycrystalline Ti-6Al-4V composed of micron-sized grains [1], in each of which a large number of slip bands can be clearly recognized. With its length of hundreds of micrometers and width of tens of nanometers (Fig. 3a, b), respectively, each slip band in Fig. 3a involves a large number of dislocations. Experimental analysis [14–17, 42, 43] have revealed that, upon the arrival of such a large number of dislocations at the slip-interface intersection, the strain/stress severely localizes and does not decay to zero

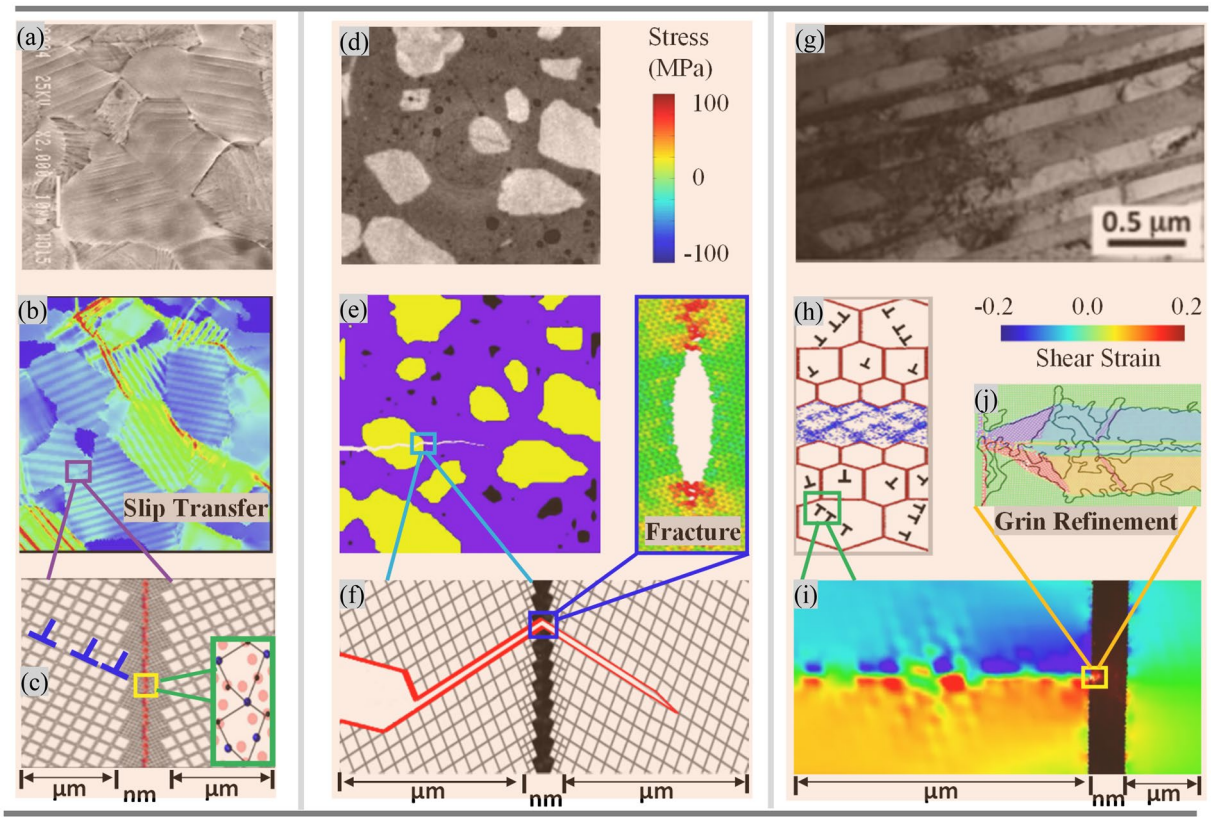

Figure 3: Multiscale mechanical behavior in three representative materials and the corresponding computer models for simulating such behavior: (a–c) the slip transfer in a plastically deformed polycrystalline Ti-6Al-4 V and the CAC model for simulating the slip-GB reactions; (d–f) the microstructure of a multiphase aggregate together with the CAC model for simulating the crack deflection at the buried interface; (g–h) the microstructure of metallic composites fabricated through ARB and the CAC model for simulating the dissimilar metal bonding process in ARB.

even at tens of microns away from the slip-GB intersection. We believe that such μm-long-range internal stresses together with the atomic-level GB geometries are the two key factors controlling the slip-interface reaction and the subsequent structure changes (cross-slip, transmission mode selection [90], twinning/PT nucleation, variant selection and growth [15]). A simultaneous incorporation of these two factors into one multiscale model like CAC (Fig. 3c) is necessary for simulating the microstructure evolution of polycrystalline alloys during plastic deformation. It will enable researchers to formulate the local stress- and even other higher order stress-informed metrics for predicting slip transfer. Such multiscale simulation-based slip transfer metrics may be expected to supplant many global resolved shear stress-based metrics [14], which are commonly used but may not have identified precise mechanisms of slip transfer.

Similar to slip transfer, fracture of a polycrystalline or multiphase aggregate can be also largely controlled by the long-range internal stress field together with the atomistic structure at the interface. As an example, Fig. 3d, e presents the cross-section of a millimeter-sized multiphase aggregate and its fracture behavior (hard phase: white in Fig. 3d and yellow in Fig. 3e; soft phase: gray in Fig. 3d and blue in Fig. 3e) [115]. When crack goes either 'from the soft to the hard phase' or 'from the hard to the soft phase' (Fig. 3e), its propagation direction slightly changes. Here we argue that the disorientation of the cleavage planes in soft/hard phases, the internal stress states upon the crack tip's arrival at the hard/soft interfaces, together with the atomistic structure at the crack-interface intersection, co-operate to engender crack deflection. To test this hypothesis, there is obviously a need to incorporate the crystallographic orientation (cleavage planes in particular), the long-range crack tip stress field (decaying as a function of $1/r^{0.5}$, r is the distance away from the crack tip), and the atomistic interface structures all in multiscale model like CAC (Fig. 3f). This is not only important for understanding the crack deflection observed here, but is also necessary for gaining knowledge on how fracture transits from 'inter-granular' to 'transgranular' in many polycrystalline materials subject to mechanical deformation.

Beyond slip transfer and fracture, another multiscale mechanical behavior of great interest is the material plasticity involved in the fabrication of layered metallic composites (Fig. 3g) through accumulative roll bonding (ARB) [2–4, 116]. The multiscale nature of dissimilar metal joining in ARB can be evidenced by: (i) the formation of μm-long dislocation-mediated slip bands in the millimeter- and μm-sized grains at an early stage of rolling (Fig. 3h); (ii) the grain refinement down to the nanoscale (Fig. 3h) and then the atomic-level interface misfit dislocation network formation at a very late stage of rolling. Understanding such a complex process through multiscale computer simulations is obviously important for correlating the ARB processing conditions with the bonding quality of the final products. Figure 3i, j presents the results from one of our recent relevant attempts along this direction through CAC simulations. It is seen that, when a large number of dislocations arrive at the interface between dissimilar metallic materials, the lattice in the adjacent layers becomes unstable. This, in turn, will activate grain refinement. Through such a preliminary attempt, CAC's unique capability on simultaneously accommodating the μm-level dislocation slip and nanoscale recrystallization is demonstrated. Its applicability to address the full complexity of the bonding process in ARB is, however, not yet benchmarked due to the lack of a robust adaptive mesh refinement (AMR) algorithm. The development of an autonomous AMR on the fly in CAC simulations is being intensively pursued [117]. Its applications in predicting the multilevel microstructure evolutions in heterogeneous materials under severe plastic deformations will be reported in the near future.

In addition to mechanical behavior, thermal transport behavior, especially phonon-mediated thermal transport, is another major concern for many engineering materials in service, such as semiconductors, oxides, ceramics, polymers, or composites comprised of these materials. In these materials, the dynamics of phonons is complicated because phonon waves, i.e., thermal-induced lattice vibrations, occur across a wide range of length scales (wavelength: *nm* for high-frequency phonons but *μm* for low-frequency phonons; mean free path: *nm* at high temperature but *μm* at low temperature). For materials dominated by phonon transport, phonon interactions with the microstructure in heterogeneous materials subject to thermal loading can be more complicated by spanning an even broader length scale. This can be elucidated by the two examples shown in Fig. 4. Figure 4a, b presents the grain structure of a polycrystalline Si (Fig. 4a) and a tri-crystalline CAC model (Fig. 4b), in which a coarse-grained (CG) description is deployed for the micron-sized grains and an atomistic resolution for the GBs. When a thermal loading (a high temperature in the middle and a low temperature on the two ends in Fig. 4b) is imposed, a μm-scale temperature gradient away from the GB together with a nm-level temperature drop near the GB (Fig. 4c) simultaneously appear on the temperature profile. Such a multiscale temperature profile is reasonable because phonons do not meet with any obstacles in the micron-sized grains but will be scattered by the crystal structure imperfection at the nanostructured GBs. Such temperature profiles can only be captured by multiscale simulations like CAC with multiple resolution co-existing in one model. More importantly, the concurrent models not only will capture the multiscale nature of the temperature profile which is considered as a collective behavior of phonons, but also can unravel the mechanism underlying the collision between the single phonon wave packet and an atomistic interface. As a demonstration, for a μm-long nanowire composed of alternative Si/SiGe layers (Fig. 4d) subject to a thermal loading, Fig. 4e–g shows the

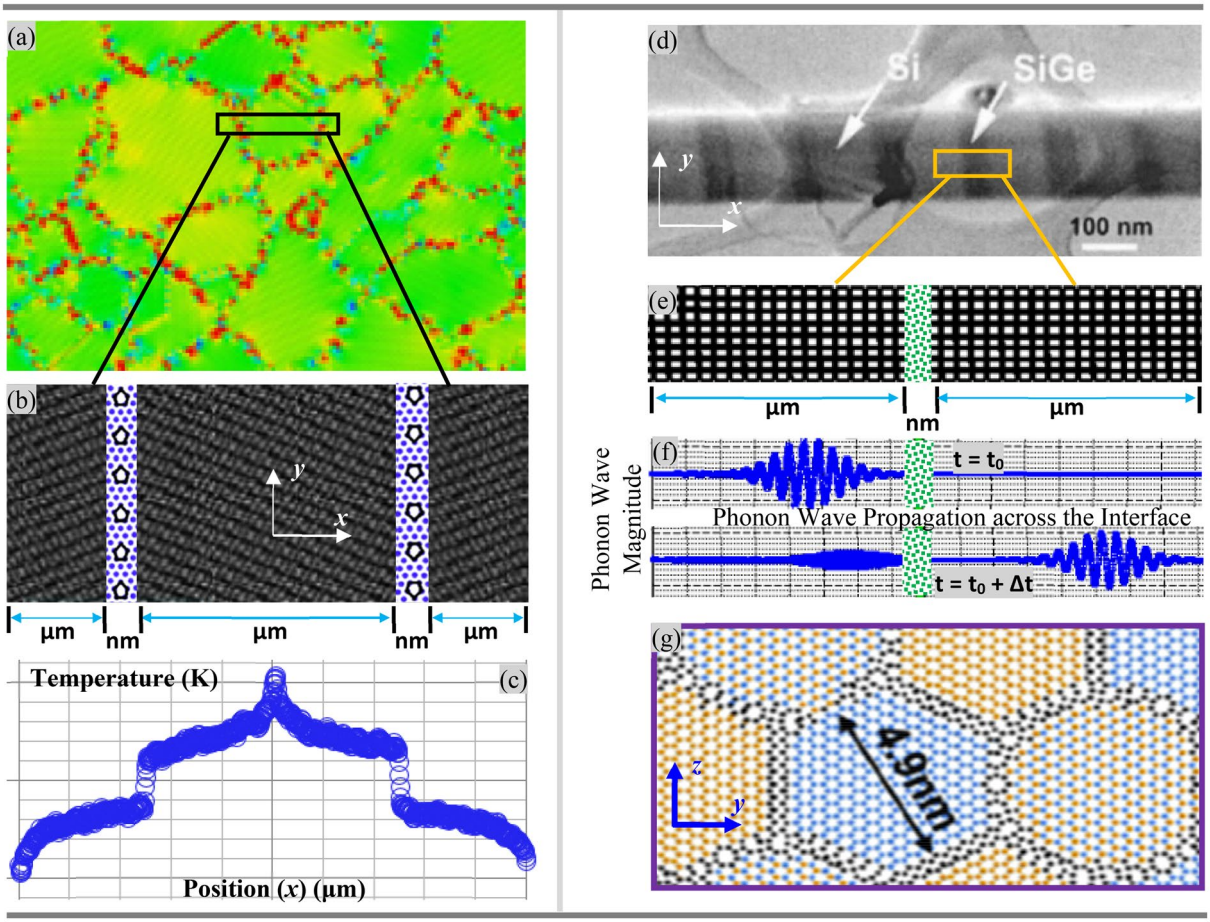

Figure 4: Multiscale thermal transport behavior in two representative materials and the corresponding computer models for simulating such behavior: (a–c) the grain structure of a polycrystalline Si, CAC model for simulating the thermal transport in a tri-crystalline sample and the temperature profile extracted from CAC simulations; (d, e) the microstructure of a μm-long nanowire composed of alternative Si/SiGe layers [6] and the corresponding CAC model; (f) CAC simulation of the phonon wave packet propagation across an interface showing the reflection and transmission; (g) the CAC simulation-predicted atomistic structure of the misfit dislocation network at the Si/SiGe interface [118].

CAC model set-up together with the simulation results on the propagation of a phonon wave packet across the Si/SiGe interface. Due to the explicit accommodation of atomistic structure at the interface, concurrent multiscale simulations will not only quantify phonon transmission/reflection coefficient but also resolve the phonon-induced interface structure reconstruction. This is usually smeared out in continuum, atomistic-informed continuum models such as BTE, but obviously cannot be simply ignored, especially when a prediction of the performance of materials subject to cyclic thermal loading is desired.

When materials containing interfaces are exposed to more aggressive environments other than stress and temperature, such as electrochemical, corrosive, ultrasonic, electromagnetic, or irradiative conditions, atomic diffusion-induced mass transport can occur and indeed control their macroscopic behavior. Taking the multilayered oxides in solid oxide fuel cells (SOFCs) and Al/Ti alloys under ultrasonic additive manufacturing (UAM) as two representative examples, we characterize the multiscale nature of atomic diffusion-induced mass transport and propose corresponding computer models for simulating them. Figure 5a shows the microstructure of a typical multilayered solid oxide, $(SrTiO_3/MgO)_n$, which contains alternative μm-thick $SrTiO_3$ and nm-thick MgO layers. At the semi-coherent interface between $SrTiO_3$ and MgO, a network of misfit dislocations (Fig. 5b) with their averaged spacing at the nanometer level is formed. Experimental measurements show that the interface misfit dislocations in layered solid oxides are favorable paths for interstitial ion hopping [122–124]. This is believed to be caused by a long-range elastic strain together with the local stress fields induced by the misfit dislocations, although a direct in situ experimental evidence is still lacking. Also, in each polycrystalline $SrTiO_3$ layer, the interstitial O^{2-} ions can be easily trapped on certain GBs but may penetrate tens of microns into the materials on the others. It suggests that the ion mobility is sensitive to either the GB structure or the local stress states or both. The interstitial

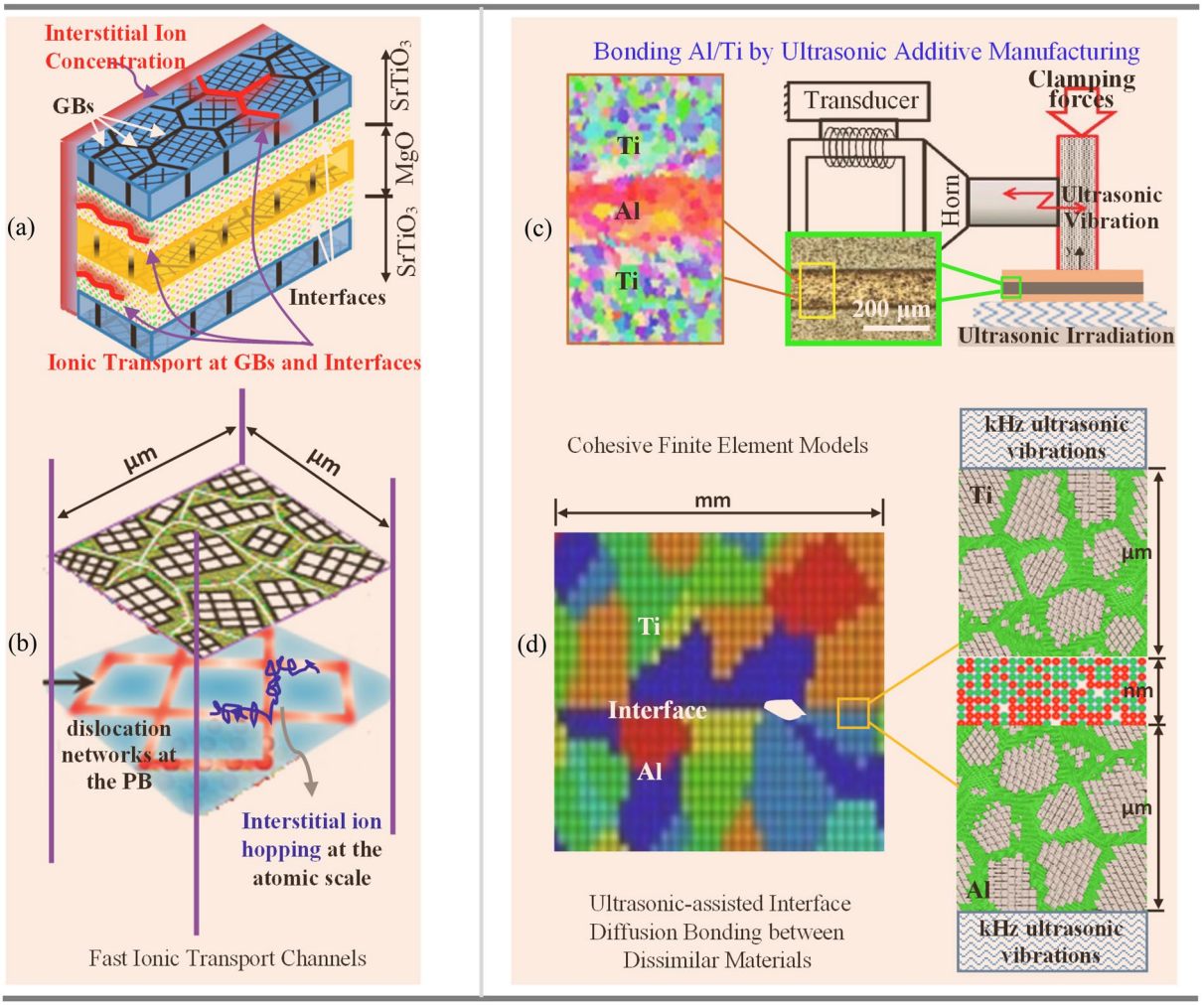

Figure 5: Multiscale mass transport behavior in two representative material systems and the corresponding computer models for simulating such behavior: (a, b) the multilevel microstructure in layered oxides, $SrTiO_3$/MgO and the proposed CAC model for simulating the interstitial ion diffusion in the complex microstructure; (c) the experimental set-up for bonding Al and Ti foils through ultrasonic additive manufacturing (UAM) [119–121]; (d) the proposed CAC model for simulating the interface bonding of dissimilar metallic materials in UAM.

ion diffusion in plastically deformed solid oxides becomes even more complicated. For instance, when the $SrTiO_3$ layer is indented, the $SrTiO_3$/MgO interface can block the dislocations and lead to the formation of a pileup as discussed before. This pileup has a long-range character and spans several microns, which can tilt the lattice structure unit, an oxygen octahedron (OCT) in the adjacent $SrTiO_3$ layer. Such OCT tilting in oxides may largely promote the interstitial ion hopping through a "cog-wheel" manner [30–34]. Clearly, the microstructure and the ionic diffusion-induced mass transport in solid oxides span from the atomistic to the micrometer level. A resemble of the multilevel microstructure together the ion diffusion dynamics under the effect of the microstructure-induced long-range internal stresses necessitates a multiscale computer models like CAC to overcome many inherent difficulties in traditional continuum or MD simulations.

Another example which can clearly demonstrate the multiscale nature of atomic diffusion-induced mass transport is the ultrasonic-assisted bonding of dissimilar materials in UAM, where the materials under a clamping force and ultrasonic vibration are bonded together through interface diffusion (Fig. 5c). The material bonding in UAM is argued to occur through four steps: surface oxide fragmentation, ultrasonic-assisted plastic flow, grain refinement, and then interface diffusion. Step-1 is less important if materials surfaces are well polished. Despite that, the occurrence of step-2 and step-4 still spans a broad range of length scales and remains not fully understood up to date in the following three aspects: (a) how does the kHz ultrasonic vibration (wavelengths: μm-mm) affect the dynamics (mobility, de-pinning from nanosized obstacles, etc.) of single dislocation lines and then their collective behavior (annihilation, junctions, pileup at GB, etc.)? (b) how does the long-range internal stress

induced by the ultrasonic-promoted dislocation accumulation at the Al/Ti interface contribute to the nanoscale twinning, phase transformations, and grain refinement nearby? (c) how does the ultrasonic-assisted motion of a large number of dislocations and their arrivals at the interface promote the inter-diffusion between Al and Ti layers? Clearly, the interface bonding process in UAM is inherently multiscale. Answering those questions necessitates concurrent multiscale simulations. Here we argue that the CAC platform provides us with a suitable, perhaps optimal approach to meet this need because it can naturally accommodate the dynamics of kHz-GHz waves, dislocations, and ion diffusion all together in one model. Figure 5d presents a multiscale model set-up to simultaneously resolve the ultrasonic-promoted plastic flow at the mesoscale, the plasticity-induced structure instability (twinning, PTs, grain refinement, etc.) at the nanoscale, and the atomic-level interface diffusion/bonding. It will elucidate the atomistic-to-mesoscale mechanisms behind the interface diffusion bonding process in UAM. Such multiscale simulations, if successful, may fill a knowledge gap in correlating the UAM processing conditions, material microstructure evolution in UAM, with the resultant bonding quality.

Future developments of multiscale modeling methodologies and potential applications

Given the extreme complexity of the interface-mediated thermomechanical behavior of advanced engineering materials, we are fully aware that a "silver bullet" for the diversity of problems under consideration in this focus issue does not yet exist. Further development of predictive multiscale materials modeling methodologies requires clear management of a variety of priorities, which include but are not limited to: (i) an incorporation of the quantum effects into the description of the mechanical, thermal, and mass transport behavior in materials, which leads to a need of, whenever possible, unifying the electronic, atomistic, and continuum description of materials in one single theoretical framework; (ii) an infusion of existing multiscale modeling methodologies with multiphysics simulations for understanding how materials respond to electro-magneto-thermo-chemo-mechanical fields because many new materials are developed with a multifunctional purpose and will be exposed to multiphysics environments (electromagnetic, irradiation, corrosive, etc.); (iii) simulations of material behavior at the μs- and μm-level as a convolution of many atomic scale events. The temporal/spatial scales of many existing multiscale methods are still not directly comparable to those of conventional experimental measurements at relatively longer time scales (seconds to hours) and larger length scales (millimeters to centimeters). We have emphasized that bottom-up, concurrent multiscale methods are more likely to yield predictive insight and understanding to guide materials design at larger scales. The development of multi-timescale algorithms is thus necessary to address this gap. A combination of existing multiscale methods with those approaches, such as accelerated molecular dynamics [125, 126], kinetic Monte Carlo (kMC) [127], nudged elastic band (NEB) [128], and quasi-static CAC [93], developed for modeling rare events might provide an alternative option to address the time scale challenge; (iv) modeling the thermomechanical or diffusional behaviors of materials at a relatively high temperature. In this situation, the short-wavelength phonon waves in the atomistic domain cannot be directly passed into the continuum domain in many existing concurrent models yet if a tri-linear shape function is employed. The reflected short-wavelength waves may alter the atomistic structure evolution at the interface. In this situation, a smooth passage of the short-wavelength waves from the atomistic to the continuum domain using a lattice dynamics-based finite element shape function [100] will be needed. Although with an increase in the computational cost, the lattice dynamics-based finite element shape functions will effectively eliminate the wave reflections at the numerical interfaces in concurrent simulations at a finite temperature; (v) the establishment of an ab initio data-driven multiscale simulation tool that can directly predict the material behavior from the electronic to the macroscopic level, because the interatomic potentials used in the existing multiscale simulation tools, may create uncertainties. The CAC simulator driven by an ab initio quality potential trained from quantum mechanical data using a machine learning algorithm may be one option to meet this need. It is under development in the group of LX and will be reported in the near future.

An extensive effort dedicated to the further development of multiscale materials modeling methodologies as outlined in the foregoing will lead to the establishment of predictive multiscale material modeling tools. This in turn, will provide decision support in the design and development of new high-performance materials for energy generation, storage and conversion, corrosion mitigation, damage and failure prevention, and thermal management. The obtained material modeling platforms will be general and the knowledge to be gained from the relevant multiscale simulations will be transferable. Their applications will not be limited in engineering sectors, but will also find widespread applications in geophysics, such as explaining and predicting the deep mantel earthquakes, or the fracture of glaciers or ice sheets in polar regions, and even the on-demand synthesis of 'born-certified' materials in deep space where many on-earth material characterization and testing facilities are simply not available. We hope this perspective together with the relevant articles collected in this focus issue will inspire researchers to develop even more advanced theories, algorithms, and software implementations toward a shift to more predictive multiphysics, multiscale materials modeling methodologies.

Acknowledgments

LX acknowledges the support of the U.S. National Science Foundation (DMR-1807545, CMMI-1930093, and CMMI-1824840) and the Extreme Science & Engineering Discovery Environment (XSEDE-TG-MSS170003 and XSEDE-TG-MSS190008). We are also grateful for the support of the U.S. National Science Foundation as a collaborative effort under Award Numbers CMMI-1761512 (YC) and CMMI 1761553 (DLM). IJB gratefully acknowledges support from the Office of Naval Research under contract N00014-17-1-2810.

Data availability

Data sharing not applicable to this article as no datasets were generated or analyzed during the current study.

Declarations

Conflict of interest On behalf of all authors, the corresponding author states that there is no conflict of interest.

References

1. M. Zhang, F. Bridier, P. Villechaise, J. Mendez, D.L. McDowell, Simulation of slip band evolution in duplex Ti-6Al-4V. Acta Mater. **58**, 1087–1096 (2010)
2. I.J. Beyerlein, N.A. Mara, J.S. Carpenter, T. Nizolek, W.M. Mook, T.A. Wynn, R.J. McCabe, J.R. Mayeur, K. Kang, S. Zheng, J. Wang, T. Pollock, Interface-driven microstructure development and ultra high strength of bulk nanostructured Cu-Nb multilayers fabricated by severe plastic deformation. J. Mater. Res. **28**(13), 1799–1812 (2013)
3. J.S. Carpenter, S.C. Vogel, J. LeDonne, D.L. Hammon, I.J. Beyerlein, N.A. Mara, Bulk texture evolution of Cu-Nb nanolamellar composites during accumulative roll bonding. Acta Mater. **60**, 1576 (2012)
4. I.J. Beyerlein, N.A. Mara, J. Wang, J.S. Carpenter, S.J. Zheng, W.Z. Han, R.F. Zhang, K. Kang, T. Nizolek, T.M. Pollock, Structure-property-functionality of bimetal interface. J. Mater. **64**, 1192 (2012)
5. I.J. Beyerlein, M.J. Demkowicz, A. Misra, B.P. Uberuaga, Defect-interface interactions. Prog. Mater Sci. **74**, 125–210 (2015)
6. D. Li, Y. Wu, R. Fan, P. Yang, A. Majumdar, Thermal conductivity of Si/SiGe superlattice nanowires. Appl. Phys. Lett. **83**(15), 3186–3188 (2003)
7. C. Dames, G. Chen, Theoretical phonon thermal conductivity of Si/Ge superlattice nanowires. J. Appl. Phys. **95**, 682–693 (2004)
8. M. Hijazi, M. Kazan, Phonon heat transport in superlattices: case of Si/SiGe and SiGe/SiGe superlattices. AIP Adv. **6**, 065024 (2006)
9. H.P. Sun, W. Tian, J.H. Haeni, D.G. Schlom, X.Q. Pan, Strain relaxation by misfit dislocations in nanoscale epitaxial ferroelectric BaTiO3 films grown on $SrTiO_3$ substrate. Microsc. Microanal. **8**(2), 1162–1163 (2002)
10. Y. Zhu, C. Song, A.M. Minor, H. Wang, Cs-corrected scanning transmission electron microscopy investigation of dislocation core configurations at a $SrTiO_3$/MgO heterogeneous interface. Microsc. Microanal. **19**, 706–715 (2013)
11. J.A. Aguiar, M. Zhuo, Z. Bi, E. Fu, Y. Wang, P.P. Dholabhai, A. Misra, Q. Jia, B.P. Uberuaga, Orientation-specific amorphization and intercalated recrystallization at ion irradiated $SrTiO_3$/MgO interfaces. J. Mater. Res. **29**(16), 1699–1710 (2014)
12. P.P. Dholabhai, G. Pilania, J.A. Aguiar, A. Misra, B.P. Uberuaga, Termination chemistry-driven dislocation structure at $SrTiO_3$/MgO heterointerfaces. Nat. Commun. **5**, 5043 (2014)
13. A. Fluri, D. Pergolesi, V. Roddatis, A. Wokaun, T. Lippert, In situ stress observation in oxide films and how tensile stress influences oxygen ion conduction. Nat. Commun. **7**, 10692 (2016)
14. Z. Zhao, T.R. Bieler, J. Llorca, P. Eisenhohr, Grain boundary slip transfer classification and metric selection with artificial neural networks. Scripta Mater. **185**, 71–75 (2020)
15. T.R. Bieler, L. Wang, A.J. Beaudoin, P. Kenesei, U. Lienert, In situ characterization of twin nucleation in pure Ti using 3D-XRD. Metall. and Mater. Trans. A **45A**, 109–122 (2014)
16. T.R. Bieler, R. Alizadeh, M. Pena-Ortega, LLorca, J., , An analysis of (the lack of) slip transfer between near-cube oriented grains in pure Al. Int. J. Plast **118**, 269–290 (2019)
17. S. Hauuala, R. Alizadeh, T.R. Bieler, J. Segurado, J. Lorca, Effect of slip transmission at grain boundaries in Al bicrystals. Int. J. Plast. **126**, 102600 (2020)
18. M.A. Kumar, N. Hilairet, R.J. McCabe, T. Yu, Y. Wang, I.J. Beyerlein, C.N. Tome, Role of twinning on the omega-phase transformation and stability in zirconium. Acta Mater. **185**, 211–217 (2020)
19. H. Chen, V. Levitas, L. Xiong, Amorphization induced by 60o shuffle dislocation pileup against tilt grain boundaries in silicon bicrystal under shear. Acta Mater. **179**, 287–295 (2019)
20. Y. Peng, R. Ji, T. Phan, W. Gao, V. Levitas, and L. Xiong An atomistic-to-microscale computational analysis of the dislocation pileup-induced local stresses near an interface in plastically deformed two-phase materials, Acta Mater., under review. (2021)
21. H. Babaei, V.I. Levitas, Effect of 60o dislocation on transformation stresses, nucleation, and growth for phase transformations between Silicon-I and Silicon-II under triaxial loading: phase field study. Acta Mater. **177**(15), 178–186 (2019)

22. V.I. Levitas, M. Javanbakht, Phase transformations in nanograin materials under high pressure and plastic shear: nanoscale mechanisms. Nanoscale **6**(1), 162–166 (2014)
23. X. Chen, W. Li, L. Xiong, Y. Li, S. Yang, Z. Zheng, D.L. McDowell, Y. Chen, Ballistic-diffusive phonon heat transport across grain boundaries. Acta Mater. **136**, 355–365 (2017)
24. A. Sood, R. Cheaito, T. Bai, H. Kwon, Y. Wang, C. Li, L. Yates, T. Bougher, S. Graham, M. Asheghi, M. Goorsky, K.E. Goodson, Direct visualization of thermal conductivity suppression due to enhanced phonon scattering near individual grain boundaries. Nano Lett **18**(6), 3466–3472 (2018)
25. S. Fujii, T. Yokoi, C.A. Fisher, H. Moriwake, M. Yoshiya, Quantitative prediction of grain boundary thermal conductivities from local atomic environments. Nat. Commun. **11**, 1854 (2020)
26. S. Kondo, T. Mitsuma, N. Shibata, Y. Ikuhara, Direct observation of individual dislocation interaction processes with grain boundaries. Sci. Adv **2**, e1501926 (2016)
27. F. Javaid, K.E. Johnns, E.A. Patterson, K. Durst, Temperature dependence of indentation size effect, dislocation pile-ups, and lattice friction in (001) strontium titanate. J. Am. Ceram. Soc. **101**, 356–364 (2018)
28. F. Javaid, E. Bruder, K. Durst, Indentation size effect and dislocation structure evolution in (001) oriented $SrTiO_3$ Berkovich indentations: HR-EBSD and etch-pit analysis. Acta Mater. **139**, 1–10 (2017)
29. J.G. Smith, D.J. Siegel, Low-temperature paddlewheel effect in glassy solid electrolytes. Nat. Commun. **11**, 1483 (2020)
30. L. Minervini, R.W. Grimes, J.A. Kilner, K.E. Sickafus, Oxygen migration in La_2NiO_4. J. Mater. Chem. **10**, 2349–2354 (2000)
31. M. Yashima, M. Enoki, T. Wakita, R. Ali, Y. Matsushita, F. Izumi, T. Ishihara, Structural disorder and diffusional pathway of oxide ions in a doped Pr_2NiO_4-based mixed conductor. J. Am. Chem. Soc. **130**, 2762–2763 (2008)
32. A. Chroneos, D. Parfitt, J.A. Kilner, R.W. Grimes, Anisotropic oxygen diffusion in tetragonal La_2NiO_4: molecular dynamics calculations. J. Mater. Chem. **20**, 266–270 (2010)
33. D. Parfitt, A. Chroneos, J.A. Kilner, R.W. Grimes, Molecular dynamics study of oxygen diffusion in Pr_2NiO_4. Phys. Chem. Chem. Phys. **12**, 6834–6836 (2010)
34. A. Kushima, D. Parfitt, A. Chroneos, B. Yildiz, J.A. Kilner, R.W. Grimes, Interstitialcy diffusion of oxygen in tetragonal La_2CoO_4. Phys. Chem. Chem. Phys. **13**, 2242–2249 (2011)
35. Y. Gao, Y. Ma, Q. An, V. Levitas, Y. Zhang, B. Feng, J. Chaudhuri, W.A. Goddard, Shear driven formation of nano-diamonds at sub-gigapascales and 300K. Carbon **146**, 364–368 (2019)
36. I.D. Noyan, G. Gadea, M. Salleras, M. Pacios, C. Calaza, A. Stranz, M. Dolcet, A. Morata, A. Tarancon, L. Fonseca, SiGe nanowire arrays based thermoelectric microgenerator. Nano Energy **57**, 492–499 (2019)
37. K. Otsuka, A. Kuwabara, A. Nakamura, T. Yamamoto, K. Matsunaga, Y. Ikuhara, Dislocaition-enhanced ionic conductivity of yttria-stablized zirconia. Appl. Phys. Lett. **82**(6), 877–879 (2003)
38. A.J. Wilkinson, G. Meaden, D.J. Dingley, High-resolution elastic strain measurement from electron backscatter diffraction patters: new levels of sensitivity. Ultramicroscopy **106**(4–5), 303–313 (2006)
39. Y. Guo, D.M. Collins, E. Tarleton, F. Hofmann, A.J. Wilkinson, T.B. Britton, Dislocation density distribution at slip band-grain boundary intersections. Acta Mater. **182**, 172–183 (2020)
40. I. Ghamarian, Y. Liu, P. Samimi, P.C. Collins, Development and application of a novel precession electron diffraction technique to quantify and map deformation structures in highly deformed materials—as applied to ultrafine-grained titanium. Acta Mater. **79**, 203–215 (2014)
41. A.C. Leff, C.R. Weinberger, M.L. Taheri, Estimation of dislocation density from precession electron diffraction data using the Nye tensor. Ultramicroscopy **153**, 9–21 (2015)
42. T.B. Britton, A.J. Wilkinson, Stress fields and geometrically necessary dislocation density distributions near the head of a blocked slip band. Acta Mater. **60**, 5773–5782 (2012)
43. Y. Guo, T.B. Britton, A.J. Wilkinson, Slip band–grain boundary interactions in commercial-purity titanium. Acta Mater. **76**, 1–12 (2014)
44. T. Lee, I. Robertson, H. Birnbaum, An in situ transmission electron microscope deformation study of the slip transfer mechanisms in metals. Metall. Trans. A **21**, 2437–2447 (1990)
45. J. Kacher, I. Robertson, Quasi-four-dimensional analysis of dislocation interactions with grain boundaries in 304 stainless steel. Acta Mater. **60**, 6657–6672 (2012)
46 A.J. Schmidt, *Optical Characterization of Thermal Transport from the Nanoscale to the Macroscale, Doctor of Philosophy, Mechanical Engineering* (Massachusetts Institute of Technology, Cambridge, 2008)
47. R.J. Stoner, H.J. Maris, Picosecond optical study of the Kapitza Conductance between metals and dielectrics at high temperature, in *Phonon Scattering in Condensed Matter VII*, vol. 112, ed. by M. Meissner, R. Pohl (Springer, Berlin, 1993), pp. 401–404
48. P.E. Hopkins, R.J. Stevens, P.M. Norris, Influence of inelastic scattering at metal-dielectric interfaces. J. Heat Transf. **130**, 022401–022401 (2008)
49. A.N. Smith, J.L. Hostetler, P.M. Norris, Thermal boundary resistance measurements using a transient thermoreflectance technique. Microscale Thermophys. Eng. **4**, 51–60 (2000)
50. D.H. Hurley, S.L. Shinde, V.E. Gusev, Lateral-looking time-resolved thermal wave microscopy. J. Korean Phys. Soc. **57**, 384 (2010)
51. D.H. Hurley, S.L. Shinde, E.S. Piekos, Interaction of thermal phonons with in- terfaces, in *Length-scale Dependent Phonon*

Interactions. ed. by L.S. Shinde, P.G. Srivastava (Springer, New York, 2014), pp. 175–205
52. M.G.S.R. Thomas, P.G. Bruce, J.B. Goodenough, AC impedance analysis of polycrystalline insertion electrodes: application to $Li_{1-x}CoO_2$. J. Electrochem. Soc. **132**(7), 1521–1528 (1985)
53. A.R.C. Bredar, A.L. Chown, A.R. Burton, B.H. Farnum, Electrochemical impedance spectroscopy of metal oxide electrodes for energy applications. ACS Appl. Energy Mater. **3**(1), 66–98 (2020)
54. D. Pergolesi, V. Roddatis, E. Fabbri, C.W. Schneider, T. Lippert, E. Traversa, J. Kilner, Probing the bulk ionic conductivity by thin film hetero-epitaxial engineering. Sci. Technol. Adv. Mater. **16**, 015001 (2015)
55. G. Holzlechner, M. Kubicek, H. Hutter, J. Fleig, A novel ToF-SIMS operation mode for improved accuracy and lateral resolution of oxygen isotope measurements on oxides. J. Anal. Spectrom **28**, 1080–1089 (2013)
56. M. Kubicek, G. Holzlechner, A. Opitz, S. Larisegger, H. Hutter, J. Fleig, A novel ToF-SIMS operation mode for sub-100nm lateral resolution: application and performance. Appl. Surf. Sci. **289**, 407–416 (2014)
57. E.B. Tadmor, M. Ortiz, R. Phillips, Quasicontinuum analysis of defects in solids. Philos. Mag. A **73**(6), 1529–1563 (1996)
58. J.Q. Broughton, F.F. Abraham, N. Bernstein, E. Kaxiras, Concurrent coupling of length scales: methodology and applications. Phys. Rev. B **60**, 2391 (1999)
59. S.P. Xiao, T. Belytschko, A bridge domain method for coupling continua with molecular dyanmics. Comput. Methods Appl. Mech. Eng. **193**, 1645–1669 (2004)
60. L.E. Shilkrot, R.E. Miller, W.A. Curtin, Multiscale plasticity modeling: coupled atomistics and discrete dislocation mechanics. J. Mech. Phys. Solids **52**(4), 755–787 (2004)
61. W. Cai, Koning, M.de, Bulatov, V.V., and Yip, S. , Minimizing boundary reflections in coupled-domain simulations. Phys. Rev. Lett. **85**(15), 3213–3216 (2000)
62. W.K. Liu, E.G. Karpov, S. Zhang, H.S. Park, An introduction to computational nanomechanics and materials. Comput. Methods Appl. Mech. Engrg. **193**, 1529–1578 (2004)
63. K. Matous, M.G.D. Geers, V.G. Kouznetsova, A. Gillman, A review of predictive nonlinear theories for multiscale modeling of heterogeneous materials. J. Comput. Phys. **330**(1), 192–220 (2017)
64. Y. Chen, J. Zimmerman, A. Krivtsov, D.L. McDowell, Assessment of atomistic coarse-graining methods. Int. J. Eng. Sci. **49**(12), 1337–1349 (2011)
65. S.S. Quek, Z. Wu, Y.W. Zhang, D.J. Srolovitz, Polycrystal deformation in a discrete dislocation dynamics framework. Acta Mater. **75**, 92–105 (2014)
66. E. van der Giessen, A. Needleman, Discrete dislocation plasticity: a simple planar model. Modell. Simul. Mater. Sci. Eng. **3**, 689–735 (1995)
67. H. Zbib, T.D. Rubia, M. Rhee, J.P. Hirth, 3D dislocation dynamics: stress-strain behavior and hardening mechanisms in fcc and bcc metals. J. Nucl. Mater. **276**(1–3), 154–165 (2000)
68. N.M. Ghoniem, S.H. Tong, L.Z. Sun, Parametric dislocation dynamics: a theromodyanmics-based approach to investigations of mesoscopic plastic deformation. Phys. Rev. B. **61**, 913 (2000)
69. V.V. Bulatov, L.L. Hsiung, M. Tang, A. Arsenlis, M.C. Bartelt, W. Cai, J.N. Florando, M. Hiratani, M. Rhee, G. Hommes, T.G. Pierce, T.D. Rubia, Dislocation multi-junctions and strain hardening. Nature **440**, 1174–1178 (2006)
70. A.M. Hussein, S.I. Rao, M.D. Uchic, D.M. Dimiduk, J.A. El-Awady, Microstructurally based cross-slip mechanisms and their effects on dislocation microstructure evolution in fcc crystals. Acta Mater. **85**, 180–190 (2015)
71. E. Bitzek, P. Gumbsch, Dynamics aspects of dislocation motion: atomistic simulations. Mater. Sci. Eng. A **400–401**, 40–44 (2005)
72. R. Yang, G. Chen, Thermal conductivity modeling of periodic two-dimensional nanocomposites. Phys. Rev. B **69**, 195316 (2004)
73. J. Zhou, X. Li, G. Chen, R. Yang, Semiclassical model for thermoelectric transport in nanocomposites. Phys. Rev. B **82**, 115308 (2010)
74. J. Ordonez-Miranda, R. Yang, J.J. Alvarado-Gil, A constitutive equation for nano-to-macro-scale heat conduction based on the Boltzmann transport equation. J. Appl. Phys. **109**, 084319 (2011)
75. J. Jamnik, J. Maier, Transport across boundary layers in ionic crystals Part II: stationary chemical diffusion. J. Phys. Chem. Solids **59**(9), 1555–1569 (1998)
76. M.P. Tautschnig, N.M. Harrion, M.W. Finnis, A model for time-dependent grain boundary diffusion of ions and electrons through a film or scale, with application to alumina. Acta Mater. **132**, 503–516 (2017)
77. J.P. Parras, R.A.D. Souza, Grain-boundary diffusion of cations in fluorite-type oxides is faster but not always easier. Acta Mater. **195**, 383–391 (2020)
78. G.J. Tucker, D.L. McDowell, Non-equilibrium grain boundary structure and inelastic deformation using atomistic simulations. Int. J. Plast **27**, 841–857 (2011)
79. Y. Chen, J.D. Lee, Atomistic formulation of a multiscale field theory for nano/micro solids. Philos. Mag. **85**(33–35), 4095–4126 (2005)
80. Y. Chen, J.D. Lee, Connecting molecular dynamics to micromorphic theory I: instantaneous and averaged mechanical variables. Phys. A **322**, 359–376 (2003)

81. Y. Chen, J.D. Lee, L. Xiong, Stresses and strains at nano/micro scales. J. Mech. Mater. Struct. **1**(4), 705–723 (2006)
82. Y. Chen, Local stress and heat flux in atomistic systems involving three-body forces. J. Chem. Phys. **124**, 054113 (2006)
83 Y. Chen, Reformulation of microscopic balance equations for multiscale materials modelling. J. Chem. Phys. **130**, 134706 (2009)
84. Y. Chen, A. Diaz, Local momentum and heat fluxes in transient transport processes and inhomogeneous systems. Phys. Rev. E **94**, 053309 (2016)
85. Y. Chen, The origin of the distinction between microscopic formulas for stress and Cauchy stress. Europhys. Lett. **116**(3), 34003 (2016)
86. Y. Chen, A. Diaz, Physical foundation and consistent formulation of atomic-level fluxes in transport processes. Phys. Rev. E **98**, 052113 (2018)
87. L. Xiong, G. Tucker, D.L. McDowell, Y. Chen, Coarse grained atomistic simulations of dislocations. J. Mech. Phys. Solids **59**, 160–177 (2011)
88. L. Xiong, D.L. McDowell, Y. Chen, Nucleation and growth of dislocation loops in Cu, Al and Si by a concurrent atomistic-continuum method. Scripta Mater. **67**, 633–636 (2012)
89. L. Xiong, Q. Deng, G. Tucker, D.L. McDowell, Y. Chen, A concurrent scheme for passing dislocations from atomistic to continuum domains. Acta Mater. **60**, 899–913 (2012)
90. S. Xu, L. Xiong, Y. Chen, D.L. McDowell, Sequential slip transfer of mixed character dislocations across sigma-3 coherent twin boundary in fcc metals: a concurrent atomistic-continuum study. NPJ **2**, 15016 (2016)
91. L. Xiong, S. Xu, D.L. McDowell, Y. Chen, Concurrent atomistic-continuum simulations of dislocation-void interactions in fcc crystals. Int. J. Plast. **65**, 33–42 (2015)
92. L. Xiong, L. Rigelesaiyin, X. Chen, S. Xu, D.L. McDowell, Y. Chen, Coarse-grained elastodynamics of fast moving dislocations. Acta Mater. **104**, 143–155 (2016)
93. S. Xu, R. Chen, L. Xiong, Y. Chen, D.L. McDowell, A quasistatic implementation of the concurrent atomistic-continuum method for fcc crystals. Int. J. Plast **72**, 91–126 (2015)
94. Q. Deng, L. Xiong, Y. Chen, Coarse-graining atomistic dynamics of brittle fracture by finite element method. Int. J. Plast **26**(9), 1402–1414 (2010)
95. S. Yang, L. Xiong, Q. Deng, Y. Chen, Concurrent atomistic and continuum simulation of strontium titanate. Acta Mater. **61**(1), 89–102 (2013)
96. S. Xu, L. Xiong, Q. Deng, D.L. McDowell, Mesh refinement schemes for the concurrent atomistic-continuum method. Int. J. Solids Struct. **90**, 144–152 (2016)
97. L. Xiong, Y. Chen, Predicting phonon properties of 1D polyatomic chains through theconcurrent atomistic-continuum simulations. Arch. Appl. Mech. **84**(9–11), 1665–1675 (2014)
98. X. Chen, A. Chernatynskiy, L. Xiong, Y. Chen, A coherent phonon pulse model for transient phonon thermal transport. Comput. Phys. Commun. **195**, 112–116 (2015)
99. X. Chen, A. Diaz, L. Xiong, D.L. McDowell, Y. Chen, Passing waves from atomistic to continuum. J. Comput. Phys. **354**, 393–402 (2018)
100. X. Chen, L. Xiong, D.L. McDowell, Y. Chen, Effects of phonons on mobility of dislocations and dislocation arrays. Scr. Mater. **137**, 22–26 (2017)
101. R. Gracie, T. Belytschko, Concurrently coupled atomistic and XFEM models for dislocations and cracks. Int. J. Numer. Meth. Eng. **78**(3), 354–378 (2009)
102. W. Yu, Z. Wang, S. Shen, Edge dislocations interacting with a Σ11 symmetrical grainboundary in copper upon mixed loading: a quasicontinuum method study. Comput. Mater. Sci. **137**, 162–170 (2017)
103. J. Cho, T. Junge, J.F. Molinari, G. Anciaux, Toward a 3D coupled atomistic and discrete dislocation dynamics simulation: dislocation core structures and Peierls stresses with several character angles in FCC aluminum. Adv. Model. Simul. Eng. Sci. **2**, 12 (2015)
104. G. Anciaux, T. Junge, M. Hodapp, J. Cho, J.F. Molinari, W.A. Curtin, The coupled atomistic/discrete-dislocation method in 3D, Part-I: concept and algorithm. J. Mech. Phys. Solids **118**, 152–171 (2018)
105. J. Cho, J.F. Molinari, W.A. Curtin, G. Anciaux, The coupled atomistic/discretedislocation method in 3D. Part-III: dynamics of hybrid dislocations. J. Mech. Phys. Solids **118**, 1–14 (2018)
106. L. Xiong, Y. Chen, Mulitscale modeling and simulation of single-crystal MgO through an atomistic field theory. Int. J. Solids Struct. **46**(6), 1448–1455 (2009)
107. L. Xiong, Y. Chen, J.D. Lee, Atomistic simulation of mechanical properties of diamond and silicon carbide by a field theory. Modell. Simul. Mater. Sci. Eng. **15**(5), 535 (2007)
108. S. Xu, T.G. Payne, H. Chen, Y. Liu, L. Xiong, Y. Chen, D.L. McDowell, PyCAC: the concurrent atomistic-continuum simulation environment. J. Mater. Res. **33**(7), 857 (2018)
109. H. Chen, S. Xu, W. Li, R. Ji, T. Phan, L. Xiong, A spatial decomposition parallel algorithm for a concurrent atomistic-continuum simulator and its preliminary applications. Comput. Mater. Sci. **144**, 1–10 (2018)
110. Y. Chen, S. Shabanov, D.L. McDowell, Concurrent atomistic-continuum modeling of crystalline materials. J. Appl. Phys. **126**, 101101 (2019)
111 J.G. Kirkwood, The statistical mechanical theory of transport processes I. General theory. J. Chem. Phys. **14**, 180–201 (1946)
112 J.G. Kirkwood, The statistical mechanical theory of transport processes II. Transport in gases. J. Chem. Phys. **24**, 72–76 (1947)

113 J.G. Kirkwood, J.H. Irving, The statistical mechanical theory of transport processes. IV. The equations of hydrodynamics. J. Chem. Phys. **14**, 817–829 (1950)
114 J.G. Kirkwood, R.J. Bearman, Statistical mechanics of transport processes. XI. Equations of transport in multicomponent systems. J. Chem. Phys. **17**, 136–145 (1958)
115. Y. Chen, A. Eskandarian, M. Oskard, J.D. Lee, Meshless simulation of crack propagation in multiphase materials. Theoret. Appl. Mech. **45**, 13–17 (2006)
116. I.J. Beyerlein, J.R. Mayeur, S. Zheng, N.A. Mara, J. Wang, A. Misra, Emergence of stable interfaces under extreme plastic deformation. Proc. Natl. Acad. Sci. **111**(12), 4386–4390 (2014)
117. T. Phan, A. Gupta, L. Xiong, and G. Tucker, Mechanistically-informed constitutive law development for slip transfer using multiscale materials modeling, the Platform for Advanced Scientific Computing Meeting, July 5–9 (invited) (2021)
118. S. Xu, Y. Li, Y. Chen, Si/Ge (111) semicoherent interfaces: responses to an in-plane shear and interactions with lattice dislocations. Phisca Status Solidi B **257**(12), 2000274 (2020)
119. R.R. Dehoff, S.S. Babu, Characterization of interfacial microstructures in 3003 aluminum alloy blocks fabricated by ultrasonic additive manufacturing. Acta Mater. **58**(13), 4305–4315 (2010)
120. N. Sridharan, P. Wolcott, M. Dapino, S.S. Babu, Microstructure and texture evolution in aluminum and commercially pure titanium dissimilar welds fabricated using ultrasonic additive manufacturing. Scr. Mater. **117**, 1–5 (2016)
121. P.J. Wolcott, N. Sridharan, S.S. Babu, A. Miriyev, N. Frage, M.J. Dapino, Characterization of Al-Ti dissimilar material joints fabricated using ultrasonic additive manufacturing. Sci. Technol. Weld. Join. **21**(2), 114–123 (2016)
122. C. Korte, A. Peters, J. Janek, D. Hesse, N. Zakharov, Ionic conductivity and activation for oxygen ion transport in superlattices-the semicoherent multilayer system YSZ (ZrO_2+9.5 mol% Y_2O_3)/Y_2O_3. Phys. Chem. Chem. Phys. **10**, 4623–4635 (2008)
123. M. Sillassen, P. Eklund, N. Pryds, E. Johnson, U. Helmersson, J. Bottiger, Low-temperature superionic conductivity in strained yttria-stabilized zirconia. Adv. Func. Mater. **20**, 2071–2076 (2010)
124. H. Aydin, C. Korte, M. Rohnke, J. Janek, Oxygen tracer diffusion along interfaces of strained Y_2O_3/YSZ multilayers. Phys. Chem. Chem. Phys. **15**, 1944–1955 (2013)
125. A.F. Voter, Hyperdynamics: accelerated molecular dynamics of infrequent events. Phys. Rev. Lett. **78**, 3908 (1997)
126. X.M. Bai, A.F. Voter, R.G. Hoagland, M. Nastasi, B.P. Uberuaga, Efficient annealing of radiation damage near grain boundaries via interstitial, emission. Science **327**(5973), 1631–1634 (2010)
127. H. Xu, Y.N. Osetsky, R.E. Stoller, Self-evolving atomistic kinetic Monte Carlo: fundamentals and applications. J. Phys. **24**, 375402 (2012)
128. A. Ghasem, P. Xiao, W. Gao, Nudged elastic band method for solid-solid transition under finite deformation. J. Chem. Phys. **151**, 054110 (2019)